HIGH VOLTAGE BUCK-BOOST LED HEADLAMP DRIVER USING ALLEGRO A6271-1

By Shashank Wekhande, Vashist Bist, and Sarang Gadgil
Allegro MicroSystems

ABSTRACT

The proliferation of light-emitting diode (LED) drivers in various automotive applications over the past decade has been driven by a need for efficient lighting and aesthetics. Multiple series-connected LEDs are used for applications such as daytime running lights (DRL) and headlamps with different LED configurations and different driving currents. In such applications, buck-boost topology is commonly used to drive LEDs over a wide range of input and output voltages. This application note discusses the features and application of the Allegro A6271-1 switching LED controller in automotive high-power applications when driving a high number of LEDs. A detailed design procedure for the A6271-1 in this application as well as details about the behavior of the device during steady-state operation, transient analysis, and behavior of various protection features are also discussed.

INTRODUCTION

The A6271-1 is an automotive AEC-Q100 qualified DC-DC controller that provides a programmable constant-current output for driving high-power LEDs in series. The controller is based on a programmable fixed-frequency, peak current-mode control architecture. The A6271-1 offers an internal switching frequency dither option that helps to reduce electromagnetic interference (EMI). The DC-DC converter can be configured in various switching configurations including boost, buck-boost (V_{IN} referred boost), buck (ground referred switch), and SEPIC configuration.

The A6271-1 is rated for a maximum output voltage of 53 V which limits the operation in buck-boost mode to three series-connected white LEDs while maintaining 40 V load dump support. While a proper selection of the external MOSFET can allow for high output voltage, the output voltage is limited by the voltage rating on the LP and LN pin. This limitation can be addressed by implementing a buck-boost converter using the A6271-1 as shown in Figure 1. Theoretically, this configuration can be used for any output voltage by proper voltage rating selection of the MOSFET (SW), Diode (D_{SW}), and output capacitor (C_{OUT}) but output voltage (V_{OUT}) is ultimately limited by the maximum duty cycle of the switching converter.

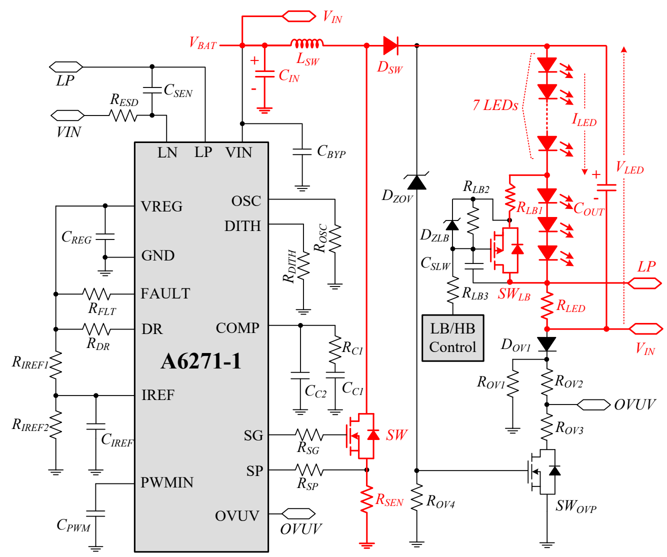

Figure 1: High-voltage buck-boost configuration using A6271-1.

In Figure 1, the inductor (L_{SW}), power MOSFET (SW), and asynchronous diode (D_{SW}) form the part of a buck-boost power stage that provides output voltage across the capacitor (C_{OUT}). High-beam or low-beam operation can be achieved by either turning on all LEDs (10 LEDs) in a string or only a few LEDs (7 LEDs) and short-circuiting the rest. An external P-channel bypass MOSFET (SW_{LB}) connected across the portion of an LED string is used for shorting the LEDs during low-beam operation. Due to the limited response time of the power stage controller, LEDs may experience a large deviation in the current during high/low-beam transitions. It is important to minimize these LED current deviations to eliminate any undesirable flicker. LEDs current deviations during high/low-beam transitions can be minimized by slowing the turn-on and turn-off rate of the bypass MOSFET (SW_{LB}). The gate-drain capacitor (C_{SLW}) across the bypass MOSFET (SW_{LB}) is added to limit the gate slew rate during the high-beam to low-beam transition to limit the inrush current. The components such as the gate protection Zener (D_{ZLB}) and resistor (R_{LB2}) are used for the gate protection of the P-channel bypass MOSFET (SW_{LB}).

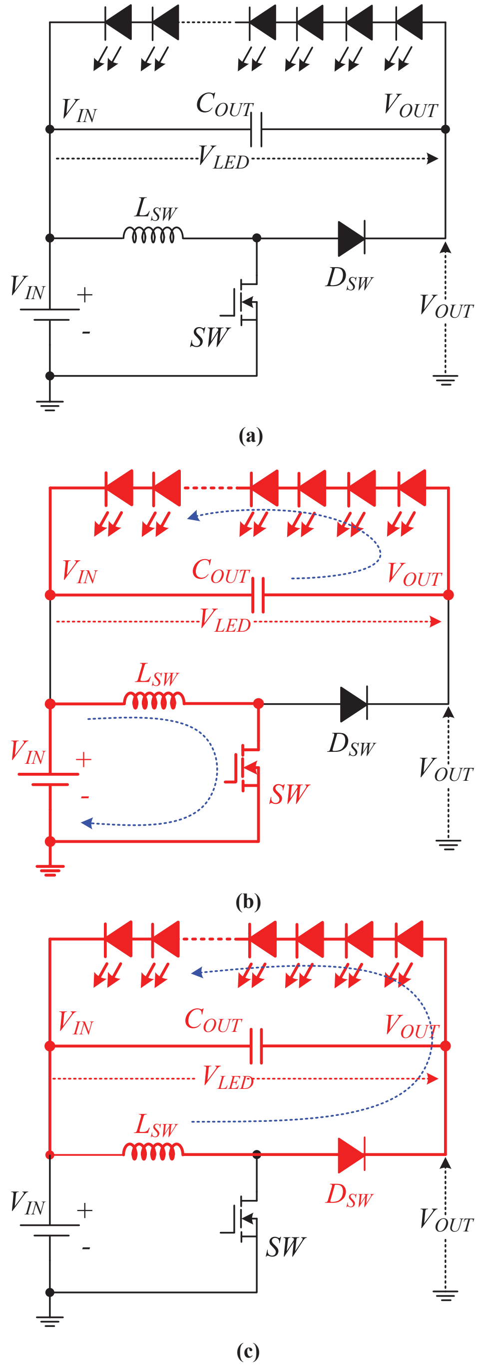

Figure 2: Buck-boost converter (a) Simplified power stage, (b) Operation during the switch-on period, (c) Operation during the switch-off period.

OPERATION

The A6271-1 is a constant frequency, peak current-mode controller. The switching frequency is set with a resistor on the OSC pin, and an optional dither feature can be enabled by connecting resistor to the DITH pin for better EMI performance.

Figure 2 (a) shows the simplified power stage of the buck-boost converter and Figure 2 (b) and Figure 2 (c) show the operation of the buck-boost converter in continuous conduction mode (CCM) during switch-on and switch-off period respectively. Figure 3 shows the waveform of the buck-boost converter in CCM mode over a complete switching cycle.

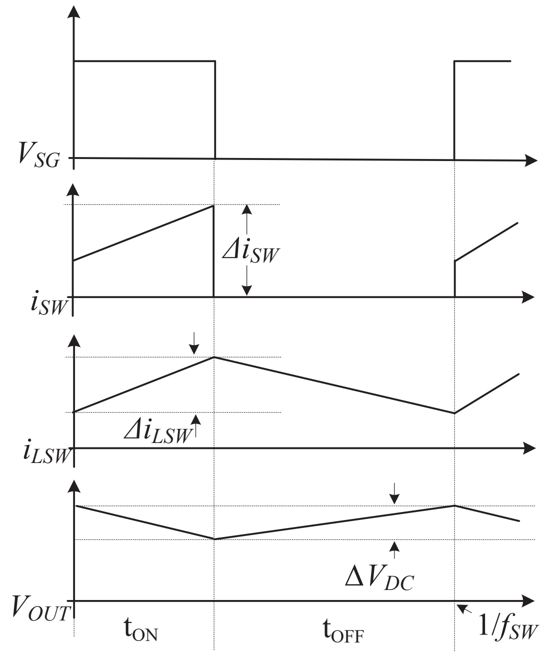

Figure 3: Waveforms of the operation of buck-boost converter in CCM.

The details on the operation of the buck-boost converter are presented below.

Mode-1 (Switch Turn-on): As shown in Figure 2 (b), when the switch (SW) turns on (t_{ON}), the energy is stored in the inductor (L_{SW}) and capacitor (C_{SW}) provides the required energy to the LEDs. During this period, the current through the switch is sensed by the sense resistor (R_{SEN} as shown in Figure 1). When the sense current becomes higher than the internal COMP reference, the controller turns off the switch.

Mode-2 (Switch Turn-off): As shown in Figure 2 (c), during the switch turn-off period (t_{OFF}), the diode (D_{SW}) conducts, and the inductor provides the required energy for charging output capacitor (C_{OUT}) and LEDs. Energy stored in the inductor (L_{SW}) is released and therefore the inductor current reduces in this mode of operation as shown in Figure 3. The output capacitor charges, and the voltage of the output capacitor (V_{OUT}) increase in this mode of operation.

Considering the input voltage as V_{IN}, output voltage as V_{OUT}, and the switch turn-on and turn-off time as t_{ON} and t_{OFF}, by balancing the volt-second across inductor L_{SW} in CCM mode is:

Equation 1:

$$V_{IN} \times t_{ON} = (V_{OUT} - V_{IN}) \times t_{OFF}$$

Replacing off time, t_{OFF} as (t – t_{ON}) and duty (D) as t_{ON}/t as,

Equation 2:

$$V_{OUT} = \left(\frac{1}{1-D}\right)V_{IN}$$

This is a typical boost converter equation showing how output voltage (V_{OUT}, with reference to ground) is linked with the input voltage (V_{IN}).

However, if the voltage across LEDs (V_{LED}) is considered, which is the difference of the output voltage (V_{OUT}) and input voltage (V_{IN}), the volt-second balance equation can be written as:

Equation 3:

$$V_{IN} \times t_{ON} = V_{LED} \times t_{OFF}$$

Replacing off time, t_{OFF} as (t – t_{ON}) and duty (D) as t_{ON}/t in Equation 3 as:

Equation 4:

$$V_{LED} = \left(\frac{D}{1-D}\right)V_{IN}$$

This shows that the voltage across the LED string (V_{LED}) varies with the input voltage in the buck-boost configuration.

The LED current is sensed through LP and LN pins by sensing the voltage across the current sense resistor (R_{LED}). The LED current is programmed by the LED sense resistor (R_{LED}) as:

Equation 5:

$$I_{LED} = \frac{V_{IDL}}{R_{LED}}$$

where, V_{IDL} is the current limit comparator reference voltage with a typical value is ~200 mV. This level can be changed for analog dimming by setting reference voltage on the IREF pin.

NOTE: It is advisable to insert a 150 Ω (R_{ESD}) resistor in series with the LN pin, as shown in Figure 1, to protect the internal ESD structures between LN and LP under certain fault conditions.

DESIGN PROCEDURE

The design procedure for the A6271-1 is as follows:

1. Configure the device switching frequency (f_{SW}) using the frequency setting resistor (R_{OSC}) as shown in Figure 1 as:

   Equation 6:

$$f_{SW} = \frac{25690}{R_{OSC}}$$

   where R_{OSC} is in kilo-ohms (kΩ) and f_{SW} is in kilohertz (kHz).

2. Select the appropriate switching frequency dither to assist in minimizing EMI emissions. In this configuration, the main oscillator can be dithered so that the energy is spread over a defined frequency band. The defined frequency band is effectively the minimum and maximum switching frequency selected. This frequency is varied above and below the selected oscillator frequency and is set via a resistor R_{DTH}. The frequency band can be selected as follows:

   Equation 7:

$$\Delta f_{SW} = \pm 22 \times \left(\frac{R_{OSC}}{R_{DTH}}\right)$$

   where Δ_{SW} is a plus/minus percentage change to the oscillator frequency f_{SW}.

3. Set the LED current (I_{LED}) by selecting voltage (V_{IREF}) on the IREF pin and LED sense resistor (R_{LED}). For this application, the IREF pin is directly connected to the VREG such that the internal current limit reference is set to the 200 mV reference level (V_{IDL}). Therefore, the LED current (I_{LED}) is selected as:

   Equation 8:

$$I_{LED} = \frac{V_{IDL}}{R_{LED}} = \frac{0.2}{R_{LED}}$$

   where I_{LED} is in amperes (A) and R_{LED} is in ohms (Ω).

   The current can also be set by using a potential divider (R_{IREF1} and R_{IREF2}) and the voltage on the IREF pin (V_{IREF}) can be adjusted as shown in Figure 1. The brightness control of LED in high-beam/low-beam operation can also be done by adjusting the I_{REF} current (i.e., V_{IREF} voltage) using an external transistor as shown in Figure 22.

4. For a 100% duty, without any potential divider (R_{IREF1} and R_{IREF2}), the soft-start time (t_{SS}) is configured by selecting the appropriate value of capacitor on the IREF pin (C_{IREF}) as:

   Equation 9:

$$C_{IREF} = \frac{t_{SS} \times 1 \times 10^{-6}}{1.2}$$

   If a potential divider (R_{IREF1} and R_{IREF2}) is used on the IREF pin, then the IREF pin capacitor (C_{IREF}) for the soft-start feature needs to be configured as per the description presented in the datasheet [1].

5. For this application, no external PWM control is used and the device is configured the 100% duty with internal PWM control. For achieving this a small 10 nF capacitor is placed on the PWMIN pin.

6. Select the output inductor (L_{SW}) as:

   Equation 10:

$$L_{SW}=\frac{V_{IN}(\min)\times D(\max)}{\Delta I_{LSW}\times f_{SW}}$$

   where V_{IN} (min) is the minimum input voltage, D (max) is the maximum duty of the converter, ΔI_{SW} is the peak-to-peak ripple current in the inductor, and f_{SW} is the PWM switching frequency. The inductor ripple current can be set to 20-40% of the average current (I_{AVG}) which is expressed as:

   Equation 11:

$$I_{avg}=\frac{D(\max)\times I_{LED}}{(1-D(\max))}$$

   Select appropriate saturation and RMS current specification for inductor design.

7. The output capacitor (C_{OUT}) is designed as:

   Equation 12:

$$C_{OUT}=\frac{I_{LED}\times D(\max)}{\Delta V_{LED}\times f_{SW}}$$

   where ΔV_{LED} is acceptable peak to peak LED voltage ripple.

8. Select switch current sense resistor and components on the COMP pin (control loop related) as per datasheet.

9. Select the appropriate setting for the overvoltage fault. Set voltage on OVUV pin at nominal operating conditions to approximately (V_{IN} – 0.5 V). A simpler way to achieve this condition is to use a diode with forward voltage drop such as 0.2 V < V_F < 0.75 V as shown in Figure 1 (Diode D_{OV1}).

   Under normal operating conditions, the MOSFET (SW_{OVP}) is off, the voltage on the OVUV pin is set by diode D_{OV1}, and resistor R_{OV1} provides a small biasing current for diode D_{OV1}. During an overvoltage event, the voltage on the OVUV pin must be 1.1 V (typical) below the input voltage (V_{IN}) to trigger the overvoltage protection. In such a scenario, the Zener diode D_{ZOV} conducts which turns on the MOSFET (SW_{OVP}). This pulls the voltage on OVUV pin below 1.1 V with respect to V_{IN} and triggers the overvoltage fault in the IC.

The values presented in the above design procedure can be selected using the standard A6271-1 design tool [2].

EXPERIMENTAL SETUP DETAILS

An experimental board to drive 10 LEDs in high-beam and 7 LEDs in low-beam for automotive headlamp application is shown in Figure 4. This application can be extended for similar applications such as the tail/stop light and daylight running lamp/position lamp. The circuit is configured in buck-boost topology to operate 8 to 18 V input voltage range with 40 V load dump. The associated schematic is shown in Figure 22 and the bill of material (BOM) is shown in Table 1.

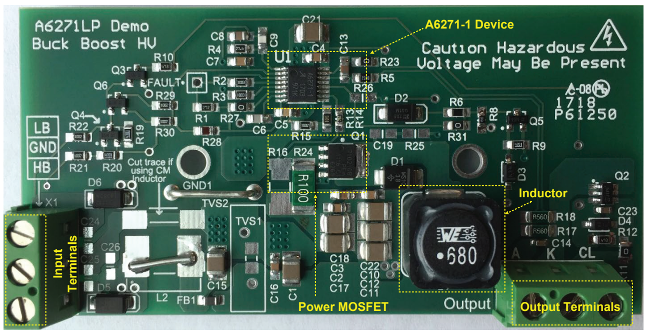

Figure 4: High-voltage experimental board using A6271-1.

STEADY-STATE OPERATION

Figure 5 and Figure 6 show the steady-state operation of the buck-boost converter using the A6271-1 device in high-beam operation at the input voltage of 12 V and 40 V respectively. As shown in Figure 5, the output voltage is maintained at 40 V for the input voltage of 12 V considering the voltage drop of 10 LEDs around ~28 V. Similarly, in Figure 6, the output voltage of the buck-boost converter is maintained at ~69 V during the load dump scenario input voltage of 40 V.

The low-beam operation of the buck-boost converter using A6271-1 at the input voltage of 12 V and 40 V is shown in Figure 7 and Figure 8 respectively. As shown in Figure 7, the output voltage is maintained at 32 V for the input voltage of 12 V considering the voltage drop of ~20 V for 7 LEDs. Similarly, in Figure 8, the output voltage of the buck-boost converter is maintained at ~60 V during the input voltage of 40 V.

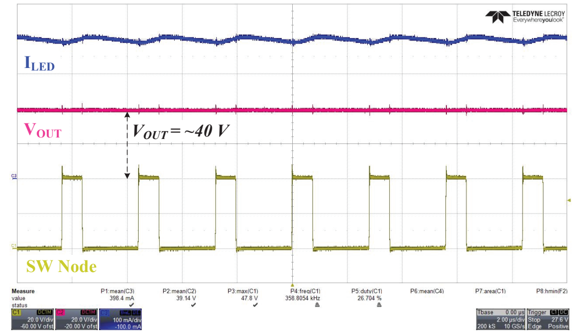

Figure 5: Steady-state operating waveforms for 10 LEDs (high-beam) for an input voltage of 12 V.

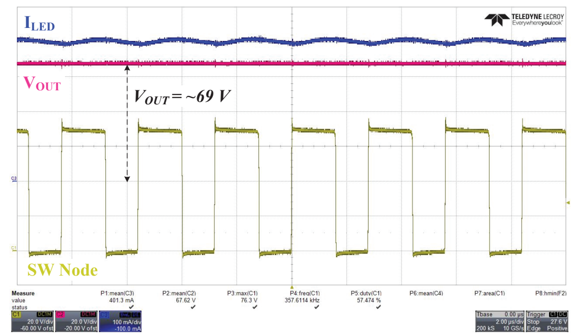

Figure 6: Steady-state operating waveforms for 10 LEDs (high-beam) for an input voltage of 40 V.

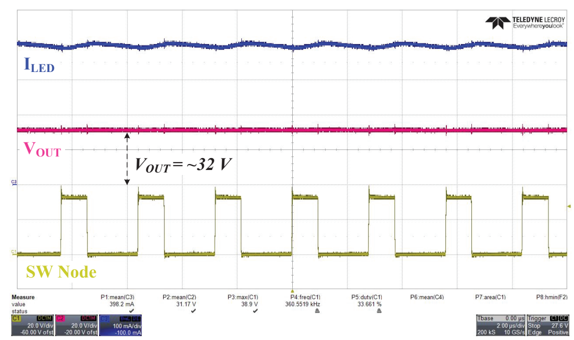

Figure 7: Steady-state operating waveforms for 7 LEDs (low-beam) for an input voltage of 12 V.

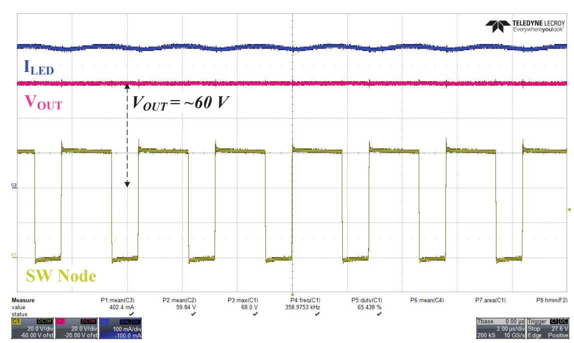

Figure 8: Steady-state operating waveforms for 7 LEDs (low-beam) for an input voltage of 40 V.

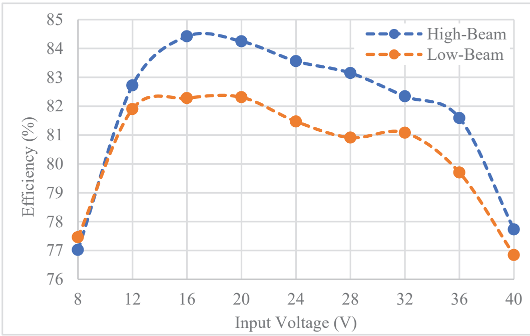

Figure 9: Plot of efficiency vs. input voltage for high-beam and low-beam operation of buck-boost converter using A6271-1.

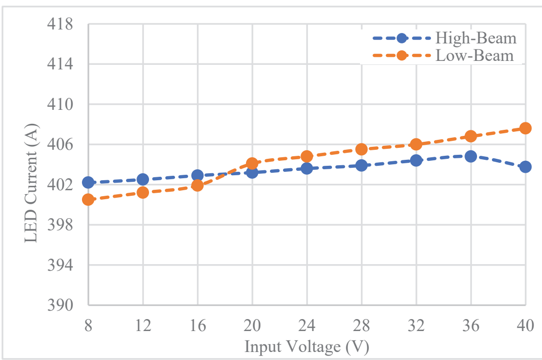

Figure 10: Plot of regulated LED current vs. input voltage for high-beam and low-beam operation of buck-boost converter using A6271-1.

The efficiency and the LED current plot with respect to the input voltage are shown in Figure 9 and Figure 10 respectively. During the low input voltage operation, the input current becomes high, which in turn increases the conduction losses of the system. Similarly, at the higher input voltage, the switching losses dominate due to the higher voltage stress on the device which reduces the overall efficiency of the system.

Figure 11 and Figure 12 show the thermal images of the buck-boost converter board operating at a rated input voltage of 12 V driving 10 and 7 LEDs respectively. As shown in these figures, the maximum temperature on the board is around 61°C / 55°C at room temperature with high-beam / low-beam operation at a rated input voltage of 12 V.

TRANSIENT OPERATION

Figure 13 and Figure 14 show the transient behavior during the high-to-low beam and low-to-high beam respectively. As shown in Figure 13, as soon as the control input (yellow) is applied, the output voltage (pink) steps down to adjust for 7 LEDs (low-beam operation). A limited inrush LED current (green) is observed within the ~12% overshoot limit. Similarly, during the low-beam to high-beam operation, an unnoticeable dip in LED current is observed and the output voltage settles within a time duration of 2 ms.

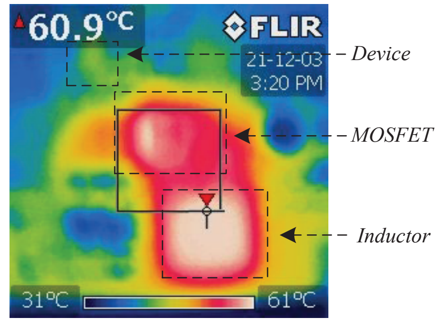

Figure 11: Thermal performance with I_{LED} = 400 mA at 12 V input and room temp for high-beam operation (10 LEDs).

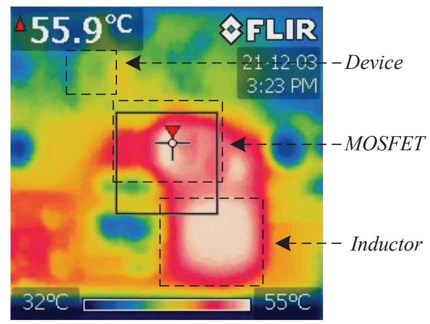

Figure 12: Thermal performance with I_{LED} = 400 mA at 12 V input and room temp for low-beam operation (7 LEDs).

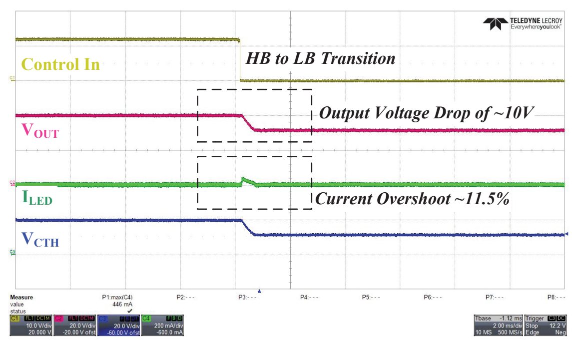

Figure 13: Transient behavior during high-beam to low-beam transition.

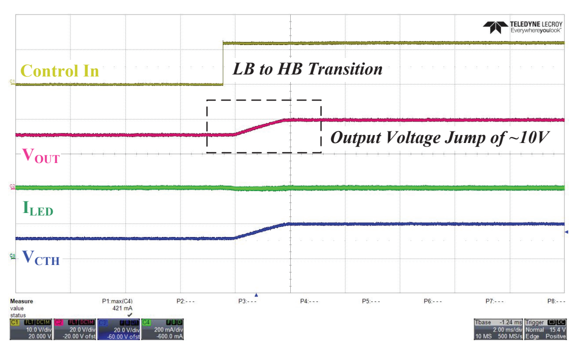

Figure 14: Transient behavior during low-beam to high-beam transition.

PROTECTIONS

The A6271-1 device integrates numerous protection schemes and is described as follows. This application does not have output undervoltage protection or overvoltage protection because of modifications required to operate the IC for higher output voltages. However, with some additional circuitry, these two protection features can be added with this high-voltage configuration as explained below.

OUTPUT OVERVOLTAGE PROTECTION (OPEN-LED): In an unwanted scenario of an open LED, the output voltage rises as the LED current feedback becomes zero. Therefore, the converter operates in an open loop and increases output voltage in an uncontrolled manner, and eventually rises to the breakdown voltage of overvoltage protection Zener diode (D_{ZOV}) as shown in Figure 1. This Zener breakdown turns on the overvoltage protection MOSFET (SW_{OVP}) and the current starts flowing through divider resistors (R_{OV2} and R_{OV3}). This creates a voltage drop and the overvoltage detection pin (OVUV) is pulled low to trigger a fault inside the IC. During this scenario, the output voltage is regulated to the OVP level. The converter returns to normal operation when the fault is removed.

Figure 15 shows OVP operation with 10 LEDs operating at the worst-case scenario of input voltage as 40 V (load dump operation). The overvoltage protection Zener diode (D_{ZOV}) is designed for ~90 V breakdown voltage. The device operation is stopped as the LED current (green) becomes zero as soon as OVP is detected in an open LED scenario. Figure 16 shows the hiccup shutdown period, as the overvoltage condition is applicable, and the driver tries to restart after the fixed hiccup period of 26.5 ms (t_{HIC}).

OUTPUT UNDERVOLTAGE PROTECTION: Additional output undervoltage protection is implemented as shown in Figure 17. In this circuit, if output voltage (V_{OUT}) goes below the Zener diode breakdown voltage (D_{ZUV}), then the output transistor (SW_{UV}) will eventually turn off and turn on the SW_{OVP} MOSFET. This in turn generates a low signal on the OVUV pin of the A6271-1 device and shuts down the operation.

INPUT UNDERVOLTAGE PROTECTION: If either input undervoltage or the regulator (V_{REG}) undervoltage scenario occurs, then the low-side MOSFET drive (SG) is disabled and FAULTn is active. Both the input voltage (V_{INUV}) and the V_{REG} voltage (V_{REGUV}) must rise above their respective turn-on thresholds to enable the IC.

TSD (Thermal Shutdown): If the junction temperature of the IC exceeds the overtemperature shutdown threshold, the low-side MOSFET drive (SG) is immediately disabled, FAULTn is active, and the IREF node (soft-start) capacitor is discharged immediately. An auto-restart is performed under control of the soft-start capacitor once the temperature drops below the overtemperature minus the hysteresis level.

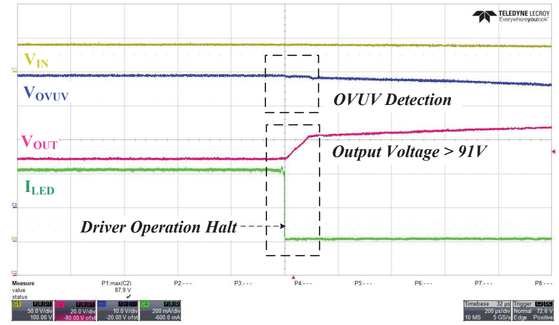

Figure 15: Overvoltage detection during open-LED operation.

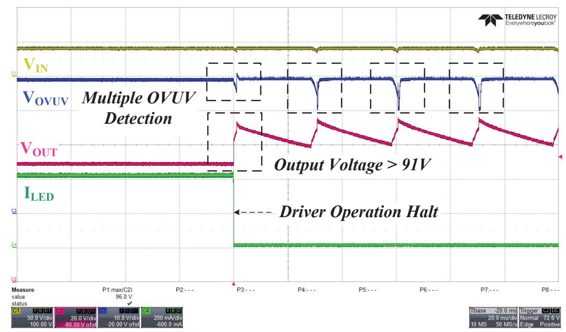

Figure 16: Hiccup operation during the overvoltage protection.

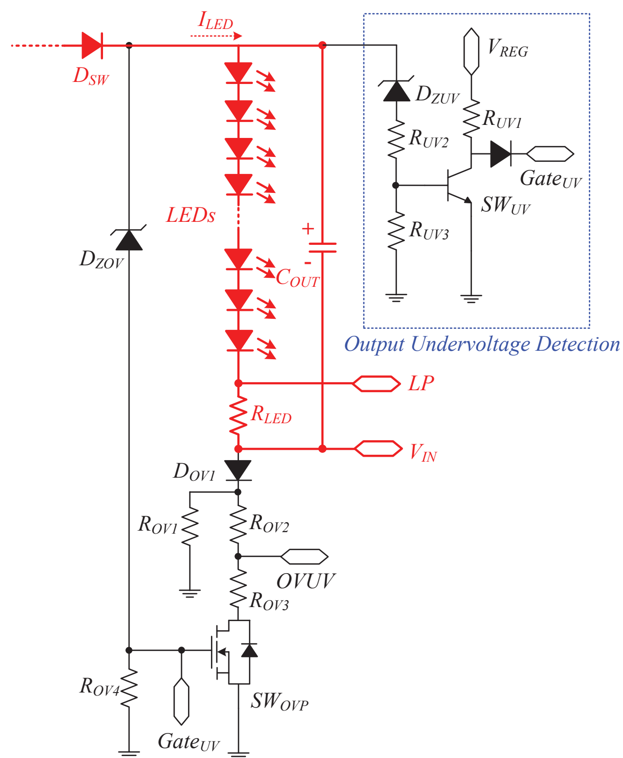

Figure 17: Additional circuit for the output undervoltage protection.

LED SHORT: In the case of an LED short, the converter will continue to operate with the remaining LEDs and regulate LED current. Figure 13 shows the transient behavior of the converter during the transition from high-beam (10 LEDs) to low-beam (7 LEDs) which is the impact of shorting 3 LEDs.

OVERLOAD PROTECTION: In case of a LED overcurrent fault, the high-side MOSFET drive (PWMOUT) and the low-side MOSFET drive (SG) are disabled after two fault mask switching cycles, FAULTn is active, the IREF node (soft-start) capacitor is discharged, then the hiccup timer (t_{HIC}) is initiated for a period of 26.5 ms. After the hiccup period, an auto-restart is performed under the control of the soft-start capacitor.

IMPACT OF SLEW RATE CONTROL

The slew rate control of the p-channel bypass MOSFET (SW_{LB}) is required to limit the inrush current in the LEDs during the high-beam to low-beam transition (turn-on of SW_{LB}). Figure 18 shows the high-beam to low-beam transition without any slew rate control on the P-channel bypass MOSFET (SW_{LB}). As shown in this figure, a very high inrush current is observed, since the inductance on the load path (LEDs) is very minimal. The slew rate of the gate voltage (yellow) and source voltage (blue) is very fast which leads to a high inrush current and eventually trips the overcurrent fault.

The slew on the bypass MOSFET can be added either by addition of the gate-source capacitance or the gate-drain capacitance. The addition of gate-source capacitance leads to a slower gate voltage rise of the MOSFET due to the extra time required to charge the additional capacitor. Figure 19 shows the waveforms with added 1 µF capacitor between the gate-source of the bypass MOSFET. As shown in this figure, the gate voltage (yellow) slew becomes very slow, and a noticeable impact can be seen in the slew of the source voltage. A current overshoot of ~23% is observed for a high value of added gate-source capacitor.

A better approach of controlling the bypass MOSFET drain-source voltage slew rate is to control the operation in the Miller region which can be done by adding the capacitance on the gate-drain pins of the bypass MOSFET. Figure 20 and Figure 21 show the impact of the addition of 100 nF and 47 nF capacitors on the gate-drain pin of the P-channel bypass MOSFET (SW_{LB}). The source pin slew rate (blue) is ~1000 µs (Figure 20) for a 100 nF gate-drain capacitor and ~500 µs (Figure 21) for a 47 nF gate-drain capacitor. The current overshoot observed with a 100 nF gate-drain capacitor is around 7.25%, whereas a 14% current overshoot is observed with a 47 nF capacitor on the gate-drain pin. As depicted here, the drain-source slew rate can be directly controlled by changing the gate-drain capacitor and current overshoot can be tuned according to the requirement.

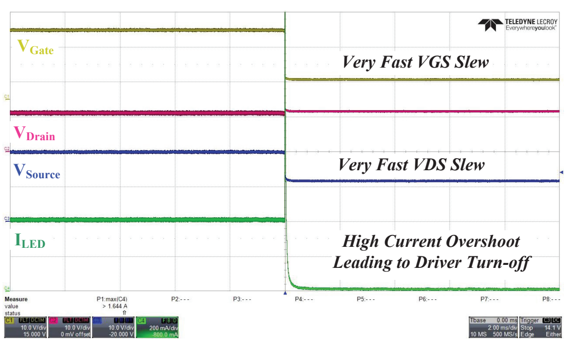

Figure 18: High-beam to low-beam transition with no added capacitance to the bypass MOSFET.

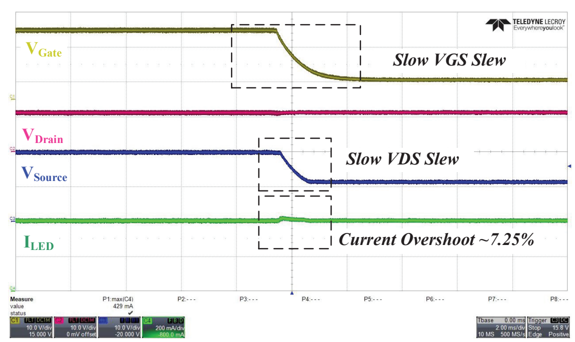

Figure 20: High-beam to low-beam transition with added gate-drain capacitance of 100 nF to the bypass MOSFET.

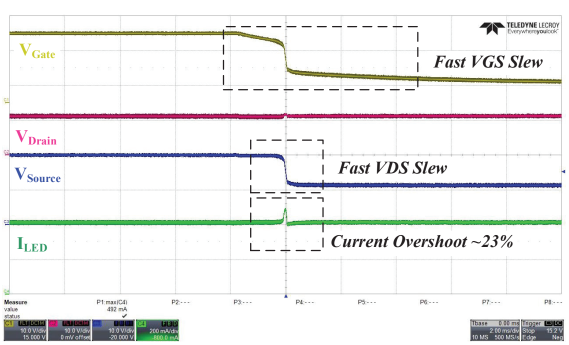

Figure 19: High-beam to low-beam transition with added gate-source capacitance of 1 µF to the bypass MOSFET.

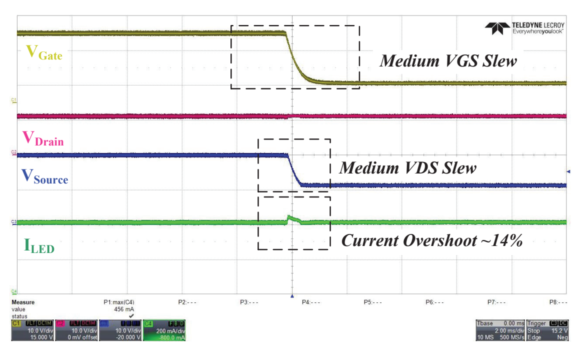

Figure 21: High-beam to low-beam transition with added gate-drain capacitance of 47 nF to the bypass MOSFET.

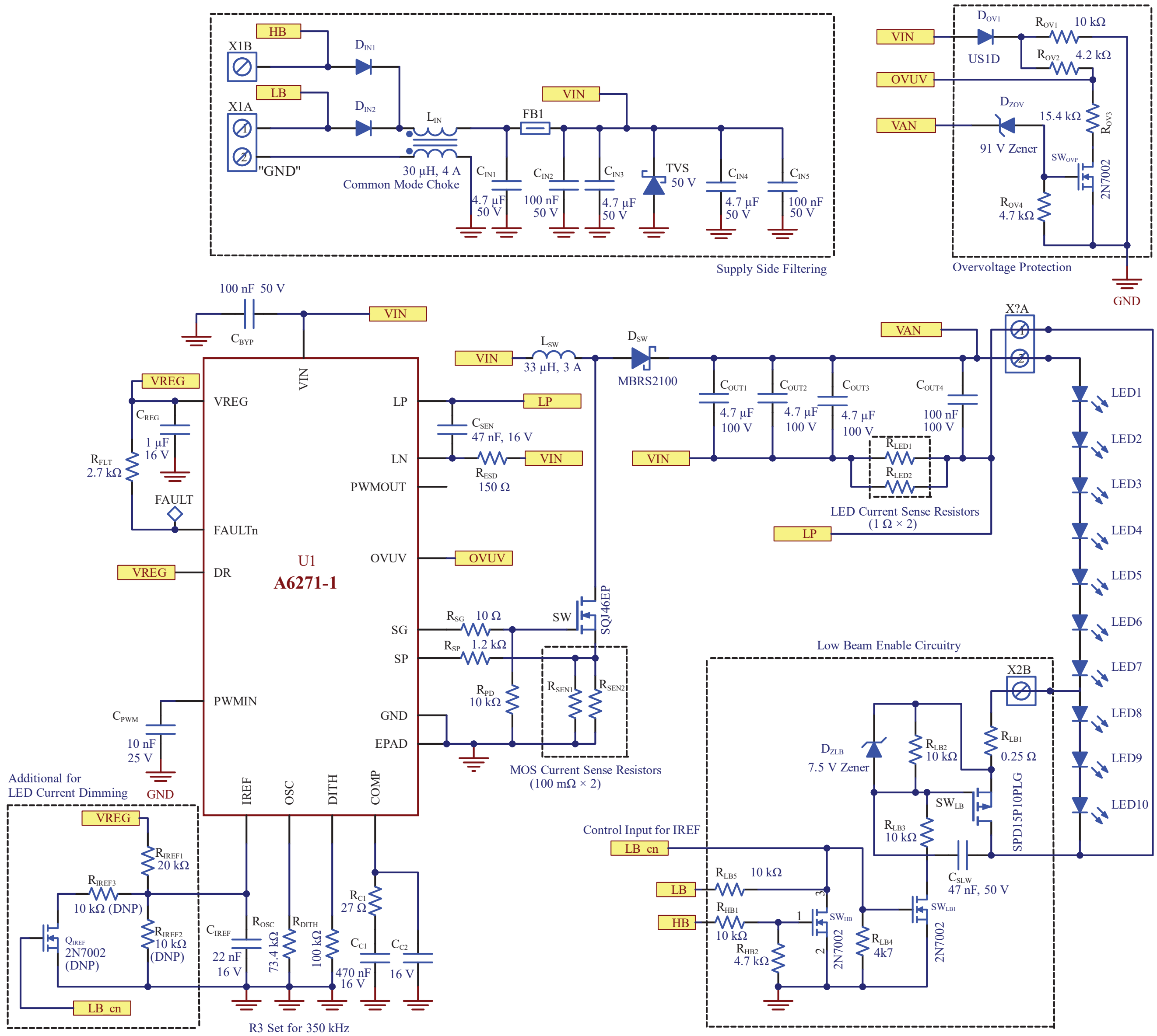

Figure 22: Schematic of the automotive headlamp application.

SCHEMATICS AND BILL OF MATERIAL

Figure 22 shows the developed schematic for the high-voltage buck-boost converter driving 10 LEDs in high-beam and 7 LEDs in low-beam with 400 mA LED current. The schematics also includes a complete circuit of the high-beam to low-beam transition with control from the 12 V battery input voltage. Additional overvoltage protection circuitry is provided for the protection of the driver in the scenario of an open-LED fault. A list of the complete bill of material (BOM) for the developed board is provided in Table 1.

CONCLUSION

The design and implementation of a high-voltage buck-boost converter using A6271-1 is presented in this application note. The following details are covered in this report:

1. Design details with a selection of various components.
2. Steady-state performance of the driver on high-beam / low-beam operation with details on thermal performance.
3. Transient behavior during the high-beam to low-beam and low-beam to high-beam operation with the impact of the slew rate control and selection of slew control parameters.
4. Various protection schemes and implementation.
5. Developed schematics and the bill of material (BOM).

REFERENCES

[1] A6271-1, Automotive High-Current LED Controller, https://www.allegromicro.com/en/products/regulate/led-drivers/led-drivers-for-lighting/a6271-1, Allegro MicroSystems, July 2019.

[2] Design Tool for High Voltage Buck-boost Converter Using A6271-1, Allegro MicroSystems, December 2021.

Table 1: Bill of Material for Automotive Headlamp Application.

Section	Designator	Description	Quantity
Power Input	D_{IN1}, D_{IN2}	Input Reverse Protection Diodes (100 V, 2 A)	2
	L_{IN}	Filter Inductor, 30 µH, 4 A	1
	C_{IN1}, C_{IN3}, C_{IN4}	Input Filter Capacitor, 4.7 µF, 50 V	3
	C_{IN2}, C_{IN5}	Input Filter Capacitor, 100 nF, 50 V	2
	TVS	50 V TVS for Load Dump Protection	1
	FB1	Surge Current Fuse	1
A6271 Comp.	U1	A6271-1 Power IC	1
	C_{BYP}	Bypass capacitor for Input Voltage, 100 nF, 50 V	1
	C_{REG}	Regulator output capacitor 1 µF, 16 V	1
	R_{OSC}	Oscillator resistor for PWM frequency set, 73.4 kΩ	1
	R_{DITH}	Dither Resistor, 100 kΩ	1
	R_{C1}	Comp pin for stabilization, 27 Ω	1
	C_{C1}	Comp pin for stabilization, 470 nF, 16 V	1
	C_{C2}	Comp pin for stabilization, 22 pF, 16 V	1
	C_{IREF}	IREF pin filter capacitor. 22 nF, 16 V	1
	R_{IREF1}, R_{IREF2}, R_{IREF3}, Q_{IREF}	Provision for reference current control, DNP	0
	R_{FLT}	Fault pin pull-up resistor, 2.7 kΩ	1
	C_{PWM}	Filter capacitor on the PWMIN pin, 10 nF, 25 V	1
	L_{SW}	Switcher Inductor, 33 µH, 3 A	1
	D_{SW}	Buck-boost converter diode, MBRS2100	1
	SW	Buck-boost converter switch, SQJ46EP	1
	R_{SEN1}, R_{SEN2}	MOSFET current sense resistors, 100 mΩ	2
	R_{SG}	Switcher gate source resistor, 10 Ω	1
	R_{PD}	Switcher gate pulldown resistor, 10 kΩ	1
	R_{SP}	SP node current limit resistor, 1.2 kΩ	1
	R_{ESD}	ESD protection for LN pins, 150 Ω	2
	C_{SEN}	Filter capacitor for current sense 47 nF, 16 V	1
	C_{OUT1}, C_{OUT2}, C_{OUT3}	Output Capacitor, 4.7uF, 100 V	3
	C_{OUT4}	Output Filter Capacitor after Rled, 100 nF, 100 V	1
	R_{LED1}, R_{LED2}	LED current sense resistor, 1 Ω each	2
LB/HB Circuit	SW_{LB}	P-channel bypass MOSFET, SPDP15P10PLG	1
	SW_{LB1}, SW_{HB}	Driving Transistors, 2N7002	2
	R_{LB1}	Power resistor, 0.25 Ω	1
	R_{LB2}, R_{LB3}, R_{LB5}, R_{HB1}	gate drive resistors, 10 kΩ each	4
	R_{LB4}, R_{HB2}	gate drive resistors, 4.7 kΩ each	2
	C_{SLW}	Gate drain slew capacitor, 47 nF, 50 V	1
	D_{ZLB}	Gate pin protection Zener diode, 7.5 V	1
OVP	D_{OV1}	Biasing diode, US1D	1
	R_{OV1}	Biasing resistor, 10 kΩ	1
	D_{ZOV}	Zener diode for OVP, 91V Zener	1
	R_{OV2}	Voltage divider for OVP, 4.2 kΩ	1
	R_{OV3}	Voltage divider for OVP, 15.4 kΩ	1
	SW_{OVP}	Driving transistor for OVP, 2N7002	1

Revision History

Number	Date	Description
–	August 28, 2023	Initial release
1	September 5, 2023	Updated introduction (page 1), Figure 3 (page 2), Equations 6, 7, and 9 (page 3), Equations 10 and 12 (page 4), and minor editorial updates